Google Scholar Crossref doi scopus

Impact factor 6.2

Geoscience Journal

ISSN:1000-8527

Indexing:

- Scopus
- Google Scholar
- DOI, Zenodo
- Open Access

www.geoscience.ac

Registered

PHYSIOCHEMICAL PROPERTIES OF AMMONIUM PENTA BORATE HEXAHYDRATE SINGLE CRYSTAL: AN EFFICIENT MATERIAL FOR OPTICAL LIMITING APPLICATIONS

A.Dilli Rani[1], C.Rathika Thaya Kumari[2], M.Nageshwari[2], P.Sangeetha[1], G.Vinitha[3], M. Lydia Caroline[4*], S.Kumaresan[1]

[1]PG and Research Department of Physics, Arignar Anna Government Arts College, Cheyyar- 604407, Tamilnadu

[2]Department of Physics, Bharath Institute of Higher Education and Research, Chennai -600073

[3]Division of Physics, School of Advanced Science, VIT University, Chennai – 600 127

[4]Department of Physics, Dr Ambedkar Govt Arts College, Vyasarpadi, Chennai – 600 039

Abstract

Ammonium Penta Borate Hexahydrate (AMPBH), an inorganic nonlinear optical (NLO) material was grown by the process of slow evaporation technique (SET) in aqueous solution. The synthesized (AMPBH) was characterized by single crystal X- ray diffraction study to affirm the structure (monoclinic), lattice parameters and space group P21/n. The functional groups in the material has been analyzed by FT-IR and FT-RAMAN studies in the range 4000 and 500 cm^{-1}. The optical absorption was determined from the recorded UV-Visible spectra and energy gap was evaluated and the value is 5.56 eV. The study on hardness infers the crystal as soft material category. The dielectric nature was examined and Jonscher's law confirms the conductivity mechanism with s=0.984. Laser damage threshold study using an Nd;YAG laser (1064nm) having pulse width 10 ns was also carried out. The luminescence nature of crystals was investigated in the range 300-800 nm and confirmed green and violet fluorescence emission spectra. Temperature of decomposition and thermal stability were investigated using TG and DTA thermal techniques. Using Gaussian beam of He-Ne laser of wavelength, the Z-scan measurement reveals negative nonlinearity i.e., self-defocussing, saturation absorption behaviour and thereby the third order nonlinear susceptibility $\chi(3)$ were also evaluated.

Keywords: Nonlinear optical crystal; Borate; Luminescence; Z-Scan;

1. Introduction

The synthesis of nonlinear optical materials to fulfill their contribution in the domain of laser technology, optical data storage, optical communication and high speed information technology is greatly needful [1,2].

Frequency conversion materials have the stability to break the restriction in optical spectrum in order to be utilized in nonlinear optical applications. The desired requirements of the NLO materials rely on large transparency range, high nonlinear susceptibility, fast nonlinear response and higher degree of laser damage threshold (LDT)[3]. Now, as the surge of polyborate salts occupying a vast position in developed applications involving fluorescence, piezoelectric, nonlinear optical (NLO) and porous materials [4-5], the versatility of borates is greatly attractive.

Inorganic borate based crystals are found to possess high transparency in the UV region and speciality of exhibiting different structures [3] emanating from special bonding properties of boron atom which coordinate with three or four oxygen atoms resulting [BO_3] or [BO_4] groups (AMPBH). Many authors reported borate based materials; Photoinduced NLO effects in doped δ-BiB_3O_6 crystals by Majchrowski et al [6]. Structure-property relationships of inorganic NLO crystal by Chang et al [7] in earlier studies in literature paved way to new series of borate based crystals [8-10]. Also Cook and Jaffe analysed the piezoelectric and electric properties of Ammonium pentaborate (AB5)[11]. C.Chen explained that the anionic group $[B_5O_6(OH_4)]^-$ or $[B_5O_8(OH_2)]^{3-}$ is responsible for NLO susceptibility of AB5[12]. Also the admiring physical properties possessed by borates namely piezoelectricity, birefringence and especially nonlinear optical nature are significantly acknowledged owing to multifunction of borate attributed to boro-oxygen (anionic groups) configurations. Researchers are meeting a great challenge in design of materials governing the borates in tuning the assembling of the anionic groups. Borates which hold on of both water molecules in it which has poly anions in its crystal structure.

Borate based NLO materials namely Potassium Borate, Potassium Pent borate (KPB), Sodium Tetra borate, Strontium Tetra borate (SrB_4o_7), Lanthanum Calcium borate ($La_2CaB_{10}O_{19}$), and Barium strontium borate has been extensively studied [13] showing stability, higher laser damage threshold

with enhance optical feature and transparent nature in UV region, provides greater difference in the electro negativity of B and O atoms which provide the basic characteristics of borates [14]. A few borate based candidate was also investigated for fourth and fifth harmonic generation using Neodymium- YAG laser.

Moreover, Boron and its compounds have a broad range of applications in industry. Especially, boric acid is a well-known medium and its potential rich chemistry has recently been discovered. In Borate materials, the boron atom typically joined with three or four oxygen atoms form [BO_3] or [BO_4] units and these units share common corners providing various building blocks with different boron atoms forming cluster in a supra molecular magnesoborate [15]. Meantime B_2O_6 unit with BO_4 tetrahedral cluster was synthesized under high pressure with more flexibility was also reported and have led to the diversity of more borate structures where as far as now more than 2000 borates were reported [15].

Borate crystals of Potassium and Ammonium are excellent non-linear optical materials which is useful in laser techniques [16] also showing lower absorption to develop Ultraviolet NLO materials. Ammonium pentaborate is a suitable solvent for metal oxides, it is utilized in the process of welding, soldering, and brazing fluxes for stainless steel or nonferrous metals [17]. The effect of shock waves to enhance the optical characteristics of Ammonium Pentaborate Hexahydrate material was studied by Anandaraj and Jothi[18].

In the present work we harvested Ammonium pentaborate hexahydrate, an alkaline borate crystals from the reaction of Ammonium carbonate, water, and boric acid. Present study includes the synthesis and growth, single crystal diffraction study, optical characterization, FTIR and FT-Raman, Laser damage threshold study, dielectric, hardness and for the first time Fluorescence and third order nonlinear characterization of AMPBH is reported, a suitable candidate for nonlinear optical applications.

2. Experimental

2.1 Material synthesis and crystal growth of AMPBH.

Ammonium Penta Borate Hexa Hydrate was synthesized from the starting materials Ammonium carbonate and boric acid of analytical grade (AR) procured from Merck Chemicals. The

calculated amount of Ammonium carbonate and boric acid were mixed in stoichiometric molar (1:2) ratio in deionized water at normal temperature. After continuous stirring for 9 hours, the homogenous solution was filtered followed by slow evaporation of the solvent to obtain the material. After 20 days optically colorless and good transparent crystals were harvested formed after spontaneous nucleation process. The photograph of as grown crystals of varying sizes are depicted in Fig. 1(a,b).

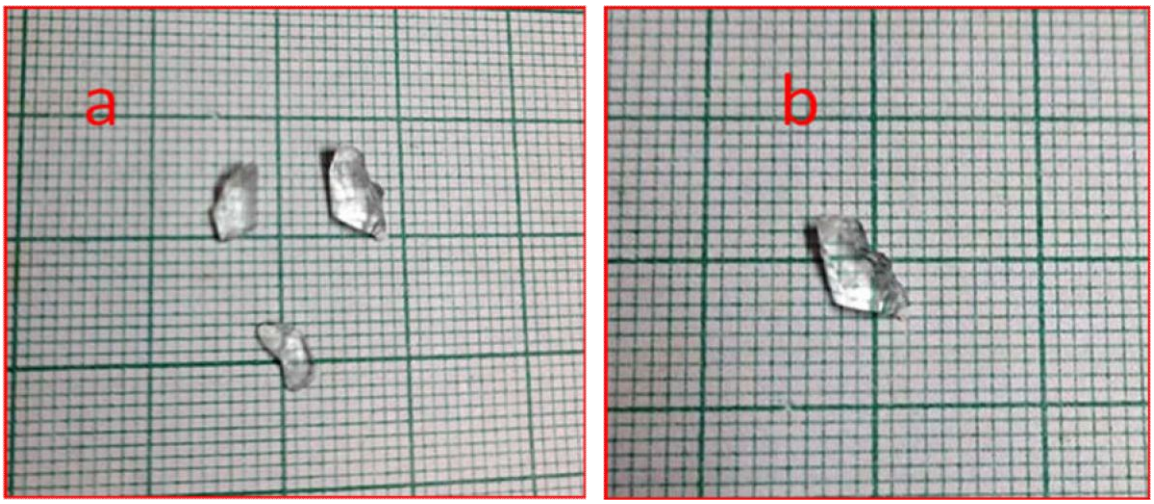

Fig. 1. (a) & (b) As grown crystal of AMPBH

3. Results and discussion

3.1 Single crystal x-ray diffraction

The grown crystal was given for single crystal X – ray diffraction to analyze the lattice parameters using BRUKER KAPPA APEX II CCD single crystal diffractometer accompanying MoKα (λ=0.71073Å). X-ray diffraction studies show that the crystal corresponds to the centrosymmetric space group of P21/n holding monoclinic system and the cell parameter values are depicted in Table 1 in accordance with reported work [18] whose structure holds a collection of five Boron with ten Oxyanions and six water molecules. The structure and crystal diffraction pattern of AMPBH is represented in Figure.2.

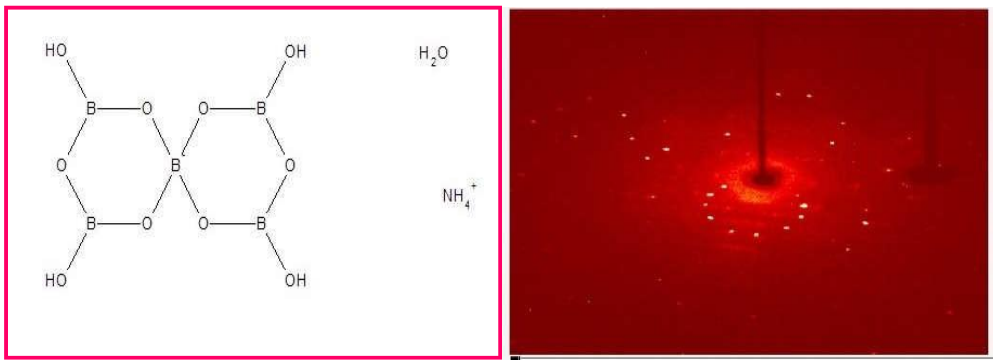

Fig. 2. Structure and Crystal diffractogram of AMPBH

Table 1. Lattice parameters of AMPBH single crystal

Cell parameters	Present work
Space group	$P2_1/n$
a (Å)	7.18
b (Å)	11.34
c (Å)	7.18
α(°)	90
β(°)	100.16
γ(°)	90
Volume $(Å)^3$	574
Crystal System	Monoclinic P

3.2 FTIR and FT-Raman Spectral Analysis

FTIR investigation on Ammonium Penta Borate Hexa Hydrate was determined from Perkin Elmer Spectrophotometer in the range 4000-500 cm^{-1} wavenumber and is depicted in Figure 3(a) and FT-Raman spectral analysis was performed using Bruker RFS 27 FT-Raman Spectrometer portrayed in Fig.3(b) respectively, where the bonding of molecule in the crystal elucidated its absorption nature.

The peak occurred in 3125-3378 cm^{-1} in IR is due to NH_4 stretching and OH asymmetric stretching. The N-H stretching vibration peaks observed at 3555 cm^{-1} (IR) and at 3551 cm^{-1}(FT-

RAMAN) respectively. The O-H (hydroxyl group) stretching of vibrations of water is seen at 3378 cm^{-1} in IR and the corresponding peak at 3344 cm^{-1} in Raman spectrum. Also the stretching and bending modes of –OH groups are observed at 2459 cm^{-1} in IR and at 2460 and 2559 cm^{-1} in FT-Raman spectrum counterpart.

The band noticed at 1653 cm^{-1} in IR is due to NH_4 asymmetric bending vibrations and the corresponding peak observed at 1602 cm^{-1} in FT-Raman. The peak at 1399 cm^{-1} in IR can be attributed to the asymmetric stretching of the BO_3 groups and the counterpart observed at 1396 cm^{-1} in FT-Raman. The borate crystals exhibit molecular vibrations in the three IR spectral regions [19].

(i) in-between 1500 and 1200 cm^{-1} pertaining to B-O stretching of trigonal B-O in BO_3.

(ii) The B-O bending vibrations of borate crystal have the absorption bands in the frequency region 782-1400 cm^{-1}.

(iii) Bending vibrations of borate appear in-between 800 and 650 cm^{-1}.

The absorption bands observed at 1354, 1248,1195,1102,1025,694 and 592 cm^{-1} in IR and peaks observed in FT-Raman spectrum counterpart at 1352, 1240, 1130, 1003, 865, 710 and 616 cm^{-1} respectively corresponds to asymmetric and symmetric stretching B-O vibrations are detailed in Table 2.

Table 2. Assignments for FTIR and FT-RAMAN

FT-IR (cm^{-1})	FT-Raman (cm^{-1})	Assignments
3378	3382	O-H Asymmetric stretching
2459	2460, 2559	Stretching and bending modes of –OH groups
1653	1602	NH_4 Asymmetric bending vibrations
1399	1396	Asymmetric stretching of B-O
1354		B-O Asymmetric stretching
1195,	1205	B-O-H bending mode
1248	1240	CH_2 Torsion
1102	1130	In plane bending B-O-H
1025	1003	B-O Terminal asymmetric stretching
922	865	B-O Ring stretching

782		B-O Ring stretching
694	710	O-B-O Ring symmetric bending
484		O-B-O Ring bending
507		O-B-O Ring bending
592	562	B-O network in pentaborate group
592	616	O-B-O Terminal bending

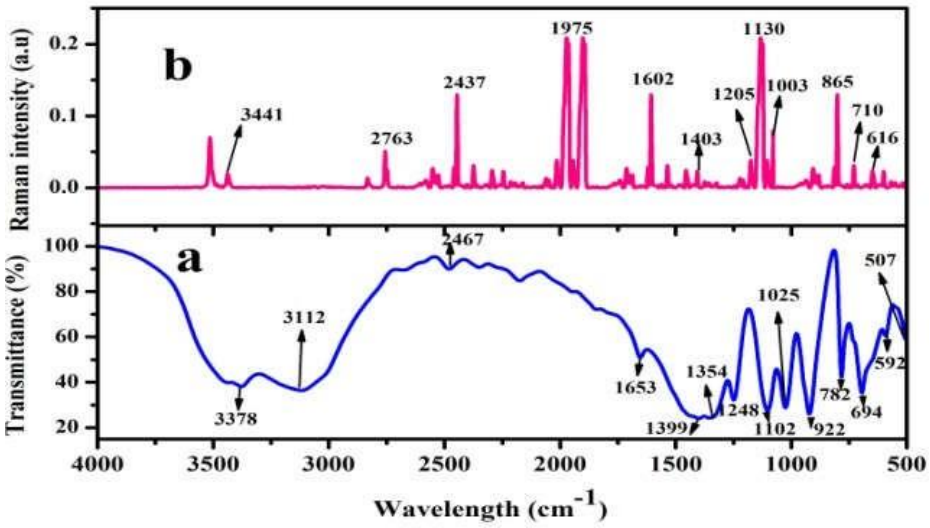

Fig.3. (a) FTIR (b) FT-Raman profile of AMPBH

3.3. UV-Visible Studies

By employing Perken-Elmer Lambda 35 UV-Vis spectrometer operated in the range 200-700 nm, the transmittance nature of the crystal was analyzed which stands as a key requirement in the field of photonics and optoelectronics[19]. The UV-Visible spectra depicted in Fig.4(a) evinces that AMPBH crystal possess low absorbance and high transmittance in the complete visible area having lower cut-off wavelength at 252 nm is the enticing factor for the materials possessing NLO properties.

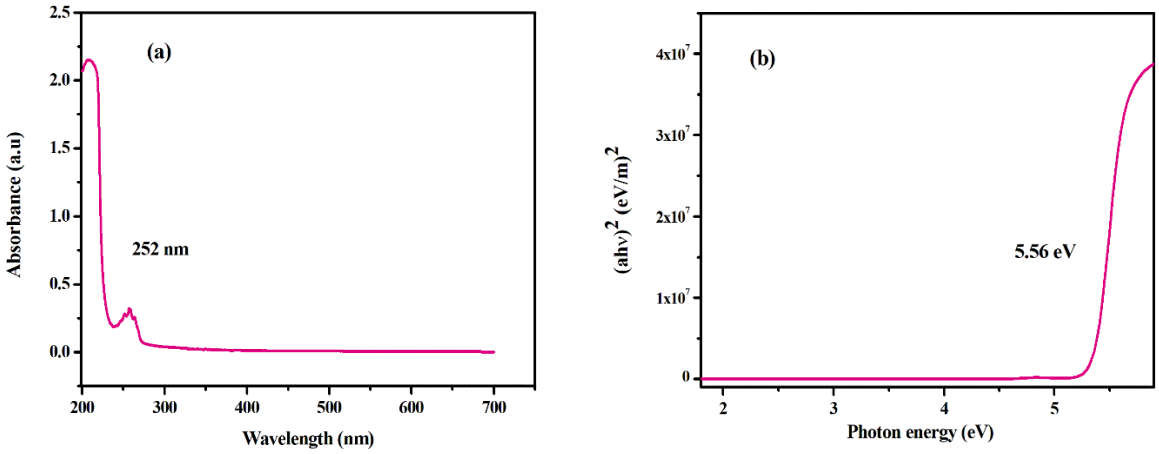

Fig.4. (a,b) UV-visible spectrum, Tauc's plot for AMPBH

3.3.1 Absorption edge and Energy gap determination

The calculated absorption values (A) was utilized to evaluate the absorption coefficient (α) utilising the following equation:

$$\alpha = \frac{2.3026\log(1/T)}{t} \qquad [1]$$

Where T, t implies the transmittance, t defines thickness of the crystal. The absorption coefficient (α) was evaluated by,

$h\upsilon\alpha = A(h\upsilon - E_g)^{1/2}$ [2]

Here A is a constant, E_g - energy gap, h infers Plank's constant, υ the frequency of the incident photon. The energy gap of AMPBH crystal was calculated from linear part of the tauc's graph plotted between $(h\upsilon\alpha)^2$ and hυ as depicted in Figure 4(b). The graph exhibits the realization of direct endorsed transition for the titled material in the range 5.0-5.6 eV. From extrapolating the straight line down to $(\alpha h\upsilon)^2 = 0$, direct electronic band gap energy E_g = 5.56eV was found. Hence, AMPBH has broad optical energy gap can be an apt candidate for UV tunable laser and NLO applications.

3.3.2. Urbach Energy

The absorption coefficient (α) as given by the Urbach equation [20].

$$\alpha(h\upsilon) = \alpha_o \exp(h\upsilon/E_u) \quad [3]$$

denote α_o as a constant, E_u pertains urbach energy, h signifies Planck's constant and υ indicates the frequency of radiation. The plot of photon energy hυ and ln(α) is shown in the profile (Figure(4c)). The crystalline feature of AMPBH is found out from the increase in value of α with photon energy hυ, depicts high crystallinity in the grown crystal. The slope 3.3316 of the linear part of the graph was calculated from log of the absorption coefficient (α) with photon energy (hυ) that explains that AMPBH has high crystalline nature [19].

The Urbach energy as evaluated from the reciprocal of the slope is 0.3002 eV. Moreover the low (0.3002 eV) estimated Urbach energy signifies minimum defect in the title ammomium borate crystal.

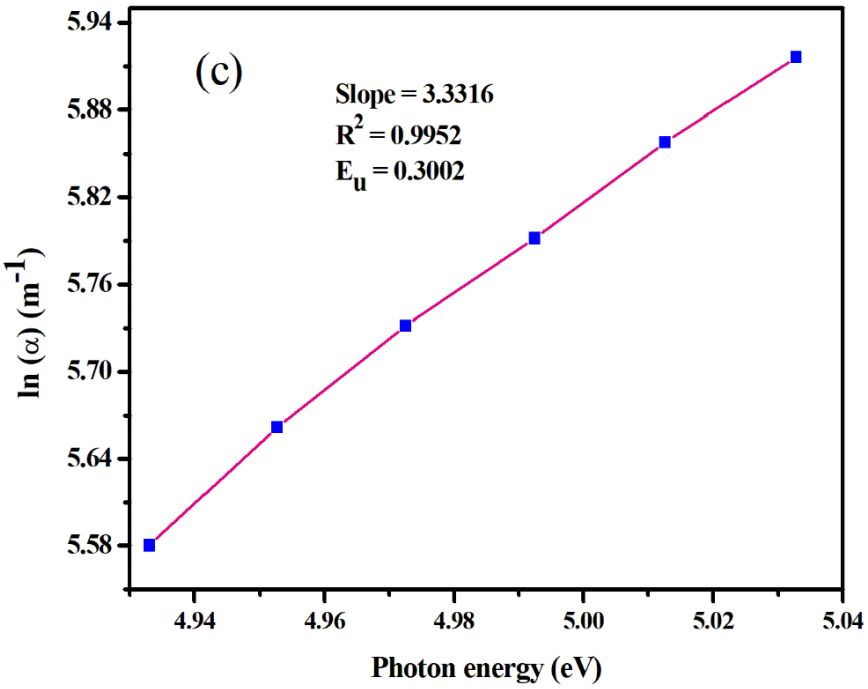

Fig.4c. Plot of ln (α) with photon energy for AMPBH

3.3.2 Optical constant determination

Using the spectra of absorption (Fig.4a), the demanding optical parameters namely transmittance, absorbance, reflectance, absorption coefficient and energy gap were valuated are essential when dealing in the field of processing, tuning, calibrating and design of technology based devices. Inclusive determination of optical constants is needed as they promote bringing the concept regarding the optical feature of the grown material. Thus the influence of extinction coefficient (K) and reflectance(R) of crystal has been studied using the computed transmittance data. The inner efficiency of the appliance too confide on the domains such as absorption coefficient and extinction coefficient (K) showing partial loss of light per unit distance in a collective medium. The extinction coefficient is evaluated using the formula:

$$K = \frac{\lambda\alpha}{4\pi} \qquad [4]$$

The graph between extinction coefficient and twain reflectance with photon energy predicts that reduction of extinction coefficient with energy [19] as shown in Fig. 5(a,b). The reflectance (R) in terms of optical absorption coefficient shown below as

$$R=1\pm\frac{\sqrt{1-\exp(-\alpha t)+\exp(\alpha t)}}{1+\exp(-\alpha t)} \qquad [5]$$

Fig. 6(a,b) depicts the twain reflectance and extinction coefficient confide on absorption coefficient. It is understood that as the values of R and K change with photon energy and also depend on absorption coefficient α, the alteration of optical constants notably the α and E_g contribute significantly towards the fabrication of optical devices [21].

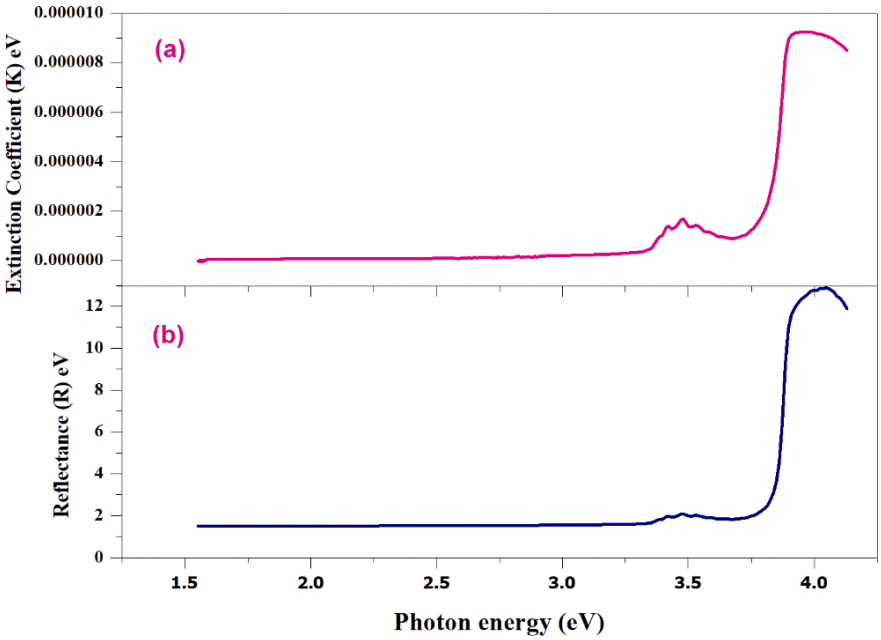

Fig. 5(a,,b) Extinction coefficient and twain reflectance(R) dependence on photon energy (hυ)

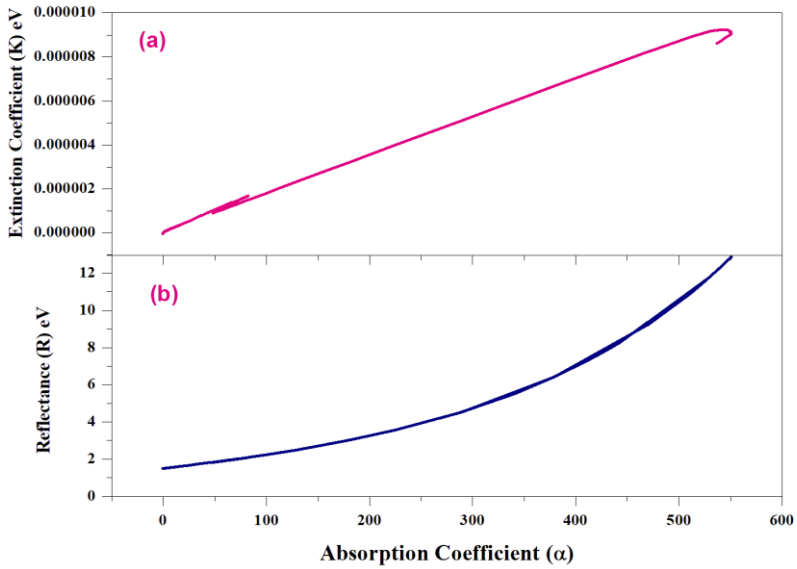

Fig. 6(a,b) Extinction coefficient and twain reflectance(R) dependence on absorption coefficient (α)

3.4. Thermo Gravimetric and Differential Thermal Analysis(TG/DTA)

Thermo gravimetric analysis (TGA) and Differential Thermal analysis (DTA) stands as a principal techniques to characterize the thermal stability of the grown material. For AMBPH the temperature withstanding point was explored by SII NANO TECHNOLOGY (MODEL TG/DTA 6200) operated between the temperature 20-800°C at a heating rate of 20°C min^{-1} under nitrogen atmosphere. Initially 2.032 mg was taken for the investigation. The TG/DTA portrayal of AMPBH is shown in Figure 7.

Two main weight losses occur between 125°C-200°C causing liberation of water molecules and NH_3 from AMPBH. The endothermic signal in DTA at around 200°C matches with TGA weight loss curve and also at around 425 °C, the DTA and TGA shows a decline at this temperature(425 °C) where the second weight loss curve ends. Further heating, third weight loss appear at 425°C and continues till 800°C with no further endothermic peaks in DTA and counterpart TGA displaying complete weight loss leading to residue of the material finally at 800 °C,

Henceforth the AMPBH crystal can be suitable for NLO applications up to 125°C.

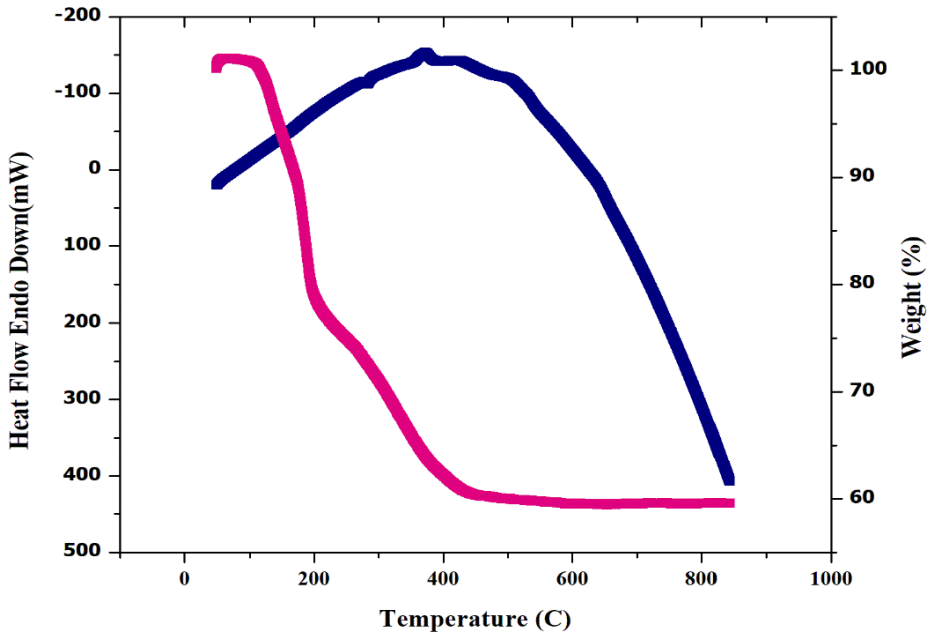

Fig.7. TG/DTA profile of AMPBH

3.5. Dielectric studies

The dielectric constant of AMPBH was estimated using the expression,

$$\varepsilon' = \frac{Cd}{A\varepsilon_0} \qquad [6]$$

Here, d, C represents the thickness and capacitance of the crystal. The change in dielectric constant and dielectric loss with frequency for various temperatures are presented in Fig. 8(a,b) which depicts that dielectric constant and loss decreases increases with frequency. For lesser frequency, dielectric constant gains larger value in view of the presence of all polarization mechanism since low dielectric constant materials has lesser measure of dipoles per unit volume when compared to the crystal possessing high dielectric constant. Hence meets the criteria in opto-electronic applications.

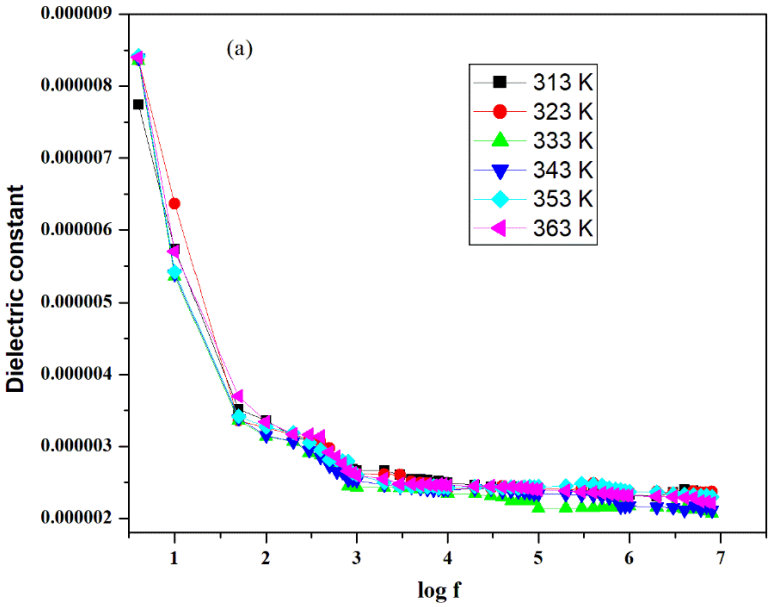

Fig.8. (a) Plot of Log f vs dielectric constant of AMPBH

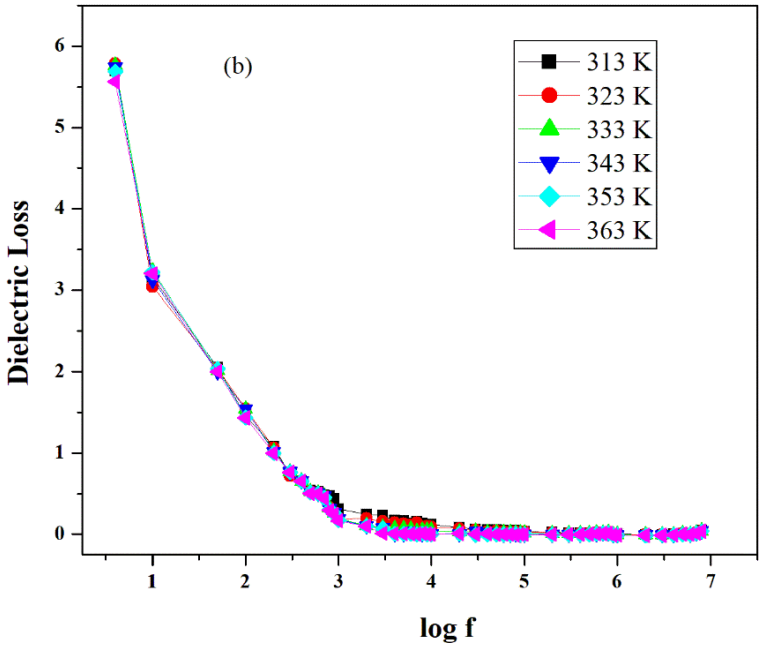

Fig.8. (b) Plot of Log f vs dielectric loss of AMPBH

3.5.1. Activation Energy

Activation energy is obtained from,

$$\sigma = \sigma_0 \exp\left(-\frac{E_a}{k_B T}\right) \quad [7]$$

Here, σ_{ac} – conductivity, T-temperature, E_a - activation energy, K_B - Boltzmann constant (1.38×10^{-23} J/K). The graph between log σ_{ac} and 1000/T is showed in Fig.9 from which the activation energy is determined by the expression from the slope in the linear portion,

E_a = - Slope x 1000 x K_B [8]

The evaluated values of activation energy was found to be 0.0241, 0.0146, 0.0112 eV at 700 Hz, 3 KHz, 20 KHz and at 3 MHz frequencies denotes that inferior values of activation energy, predicts less defects in materials pertaining to their usefulness in device fabrications.

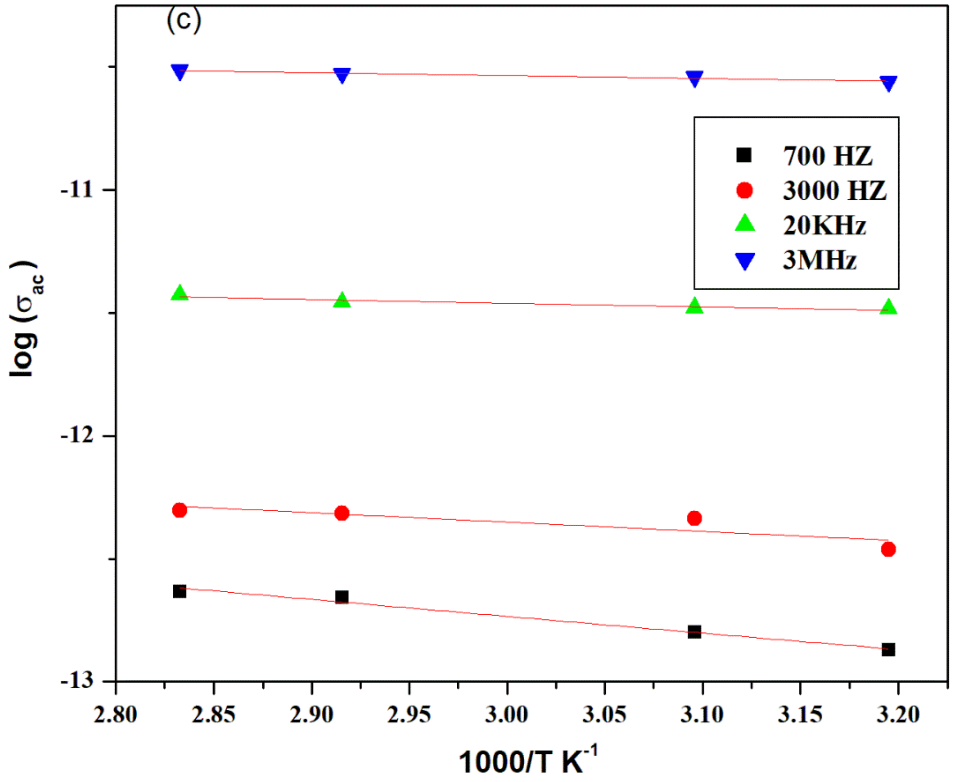

Fig.9. Plot of 1000/T verses Log σ_{ac}

3.5.2. Mechanism of Conduction-Jonscher's power law

The relationship between electrical conductivity σ_{ac} and frequency seen in various solids constituting polymers, glasses and crystals was looked over by Jonscher is well acknowledged by the power law [22],

$$\sigma_{a.c} = \sigma_{d.c} + A\omega^{S} \qquad [9]$$

, where σ_{dc} infers DC conductivity that concludes the frequency (ω)independent plateau in lower frequency, A is a constant that depends on temperature rely on polarisation, and s - power law exponent that lies in the middle $0 < s < 1$, that vary with materials. Figure 10 represent the specification of Jonscher's power law explored for the title material whose s = 0.984 established from the slope of the graph leads to the good agreement of the power law. The conduction procedure recognized from the

graph infers that AC conductivity step-up almost at higher frequency as a result of hopping mechanism [23] observed from AMPBH crystal.

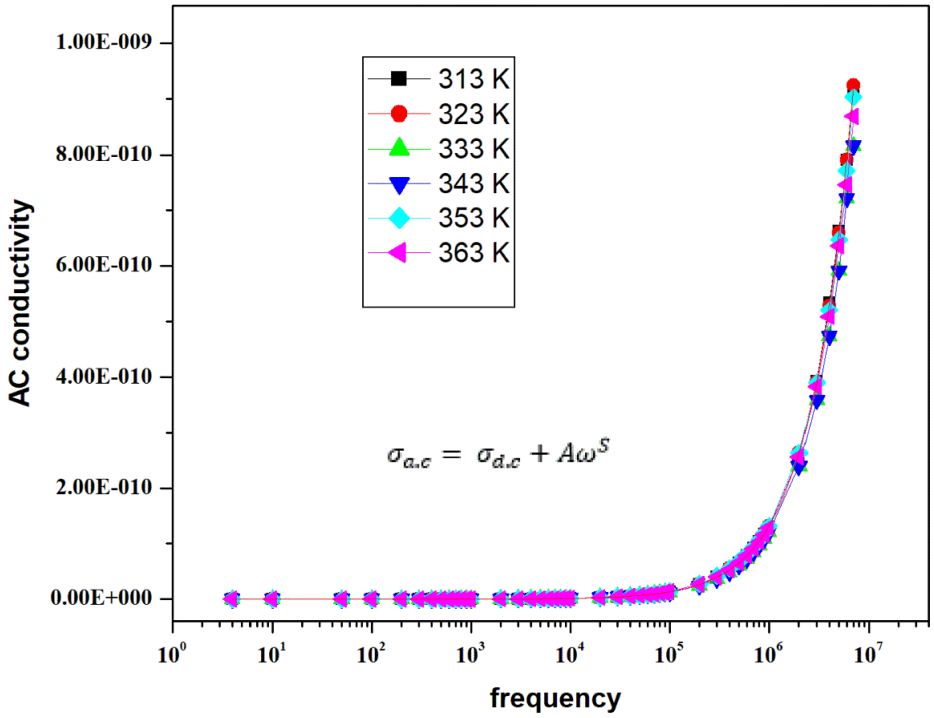

Fig.10. Plot of AC conductivity vs Frequency

3.6. Micro (mechanical) hardness studies

The microhardness study confirms the materials capacity in device fabrication by exploring the mechanical strength. The strength of the materials depends on various parameters such as lattice energy, Debye temperature, heat of formation and interatomic spacing. The MH- 112 Vicker's microhardness measurement on AMPBH crystal was done at room temperature and load of 25, 50, and 100 g were applied.

. The Vicker's hardness which connects the applied load and diagonal of the indent was evaluated using standard formula

$$H_v = 1.855\ (P/d^2) \qquad [10]$$

Where P implies applied load , d the mean length of the indenter impression , and 1.8544 is a constant. Figure 11(a) represents the dependence of hardness number (H_v) with applied load extending from 25-

100 g for AMPBH, where H_v increases with the increase in the load is observed is well considered as the reverse indentation size effect [RISE] [24,25].

The Meyer's index coefficient was calculated from Meyer's law [19], which imparts a relation between the load and indentation diagonal length,

$$P = K^1 d^n \quad [11]$$

(or)

$$\log P = \log K_1 + n \log d \quad [12]$$

Where K_1 signifies constant and 'n' denotes Meyer's index. Work hardening coefficient 'n', is checked from a plot drawn between log P vs log d as displayed in Figure 11(b). From the slope of the linear straight line the value of 'n' is 3.70. For the normal RISE behavior, the condition is n <2. When n > 2, it infers reverse RISE behavior. This is good coincidence with the experimental data pointing towards reverse RISE. As per the statement given by Onitsh [26], work hardening coefficient should be between 1 and 1.6 for harder materials and above 1.6 for softer category. Hence, AMPBH can be termed as soft material category.

$$\sigma_y = \frac{H_v}{3}(0.1)^{n'-2} \quad [13]$$

Where n′ = n+2.

A graph between the variations of load P with yield strength σ_y is calculated for AMPBH crystal (Figure 11 (c)).

The elastic stiffness constant (C_{11}) is also figured out from Wooster's empirical formula [27],

$$C_{11} = (H_v)^{7/4} \quad [14]$$

The elastic stiffness constant recognizes the nature of bonding between neighbouring atoms. A graph is between load P vs. stiffness constant C_{11} illustrated in Figure 11 (d) furnish that the stiffness constant increases with increase of load. The greater the stiffness constant C_{11} lead to the conclusion that the binding forces between the ions are quite energetic.

The Knoop's hardness number (H_K) is also determined from,

$$H_K(Kg/mm^2)=14.229\frac{P}{d^2} \quad [15]$$

From the tabulated values of load P and H_K (Knoop's hardness number), the graph is plotted (Fig. 11e). The calculated mechanical parameters are tabulated (Table 3)

3.6.1 Heys-Kendall (HK) Approach

The point of view regarding the study of HK, which initiates the determination of load independent parameter hardness[28], from the relation

$P = W + A_1d^n$, where W refers initiation of plastic (permanent) deformation (in grams). A_1 is the load-independent constant and the exponent n = 3.70. The quantities W and A_1 were concluded from the graph load P vs. d^2 as shown in Figure. 11f. The corrected load independent hardness H_{HK} value (Table 4) of AMPBH was valuated from:

$$H_{HK} = 1854.4A_1 \quad [16]$$

From the hardness analysis AMPBH crystal proves that has sufficient mechanical strength for various NLO device fabrications. The estimated mechanical parameters are listed in the Table 3.

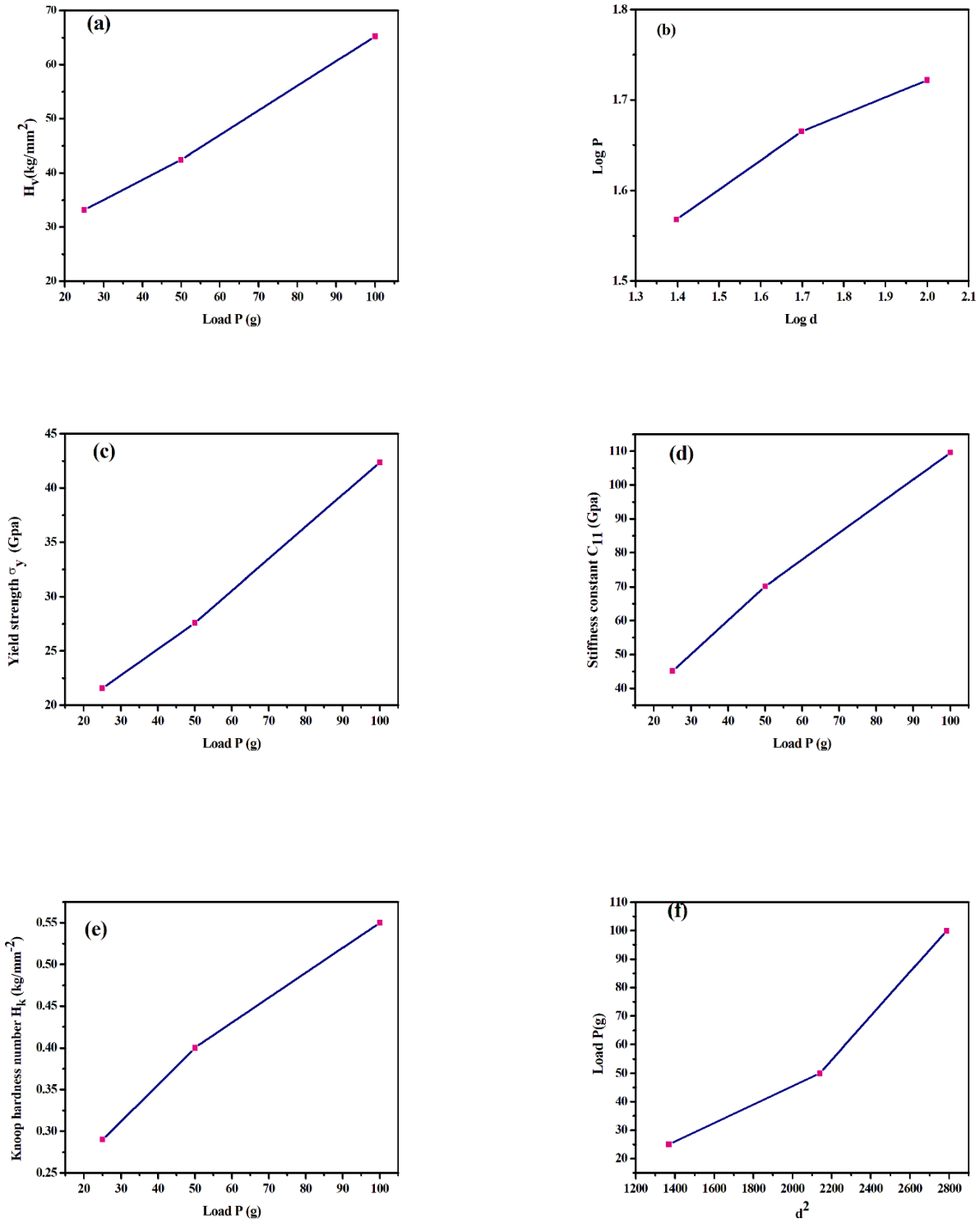

Fig.11(a,b,c,d,e)Microhardness , Meyers plot,Yield strength,Stiffness constant,Knoop's hardness number, load P vs. d^2

Table 3: Computed Mechanical parameters

load P(g)	n	H_v(kg mm^{-2})	σ_y(G Pa)	H_K(Kg/mm^2)	C_{11}(M Pa)
25	3.70	33.18	21.56	25.46	4.495
50	3.70	42.44	27.58	32.56	6.915
100	3.70	65.18	42.35	51.03	14.652

Table 4: Calculated HK constant W, A_1, and H_{HK}

HK constant	Results
Resistance Pressure(W)	-44.0682 (g)
Load independent constant (A_1)	0.0482 (g/μm^2)
Corrected load independent hardness (H_{HK})	89.38208 (g/μm^2)

3.7. Photoluminescence Studies (PL).

PL spectroscopy plays a vital role in exploring the electronic structure and assessing the transparency of the solid and discovering the energy states existing between valence band and conduction band responsible for radiative recombination [28]. The photoluminescence spectrum observed in the range 300-800 nm is delineated for AMPBH showing room temperature phosphorescence with an excitation wavelength of 253 nm using PERKIN ELMER LS45 Spectrophotometer (Figure 12). The PL spetra portrays one green fluorescence peak at 506 nm (2.45 eV) , one cyan(blue) emission peak at 463 nm (2.68 eV)and one violet fluorescence peak at 384 nm (3.23 eV) which emerges as a result of disappearance of self-trapped excitons linked with the molecular transitions within the BO_3^- group[19] makes AMPBH suitable in optical data storage devices[29].The blue phosphorescence spectra emerges as a result of high energy photons and the generation of green phosphorescence due to low energy photons [30]. In ammonium borate crystals B-O provides the π-bond orbitals and or π^* anti-bond orbitals in phosphorescent excited states that paves way to synthesize advanced class of phosphorescent materials applicable in tunable lasers[30].

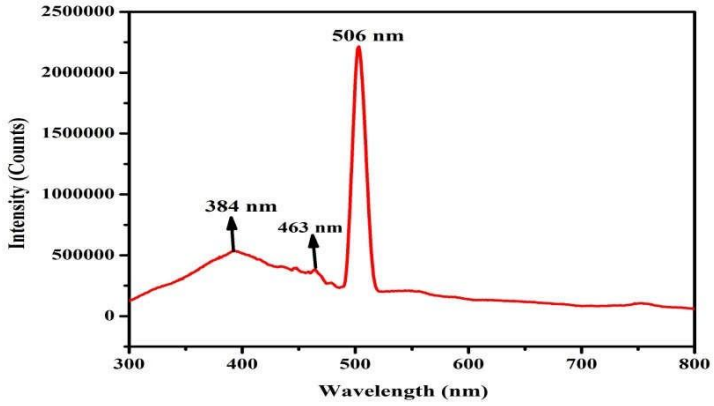

Fig.12. Emission spectrum of AMPBH

3.8. Laser Damage Threshold (LDT) Study

LDT is usually connected to rise in temperature in the materials leading to strain-induced fracture evolved by electron avalanche, multi-photon absorption and ionization processes [31]. LDT measurement was performed by Q-switched Nd:YAG laser source with primitive wavelength (1064 nm, 6 ns, 10 Hz). Multiple shot LDT equivalent of title crystal was evaluated from power density expression:

$$\text{Power density } (P_d) = E/\tau\pi r^2 \ (GW/cm^2) \qquad [17]$$

[Where E, τ, r represents input energy (mJ), pulse width (ns), radius of the laser beam spot (mm)] is 10.59 GW/cm^2, established the materials suitability for high power laser applications.

3.9. Z-Scan measurements

Highly sensitive and a standard method for determining nonlinear optical properties of materials such as solids, liquid solutions and thin films like absolute magnitude and sign of nonlinear refractive index (n_2), nonlinear absorption (NLA) and nonlinear refraction (NLR) was developed for wide applications in the field of optical imaging, multi-photon polymerization including optical switching is the method of Z-scan introduced by Sheik-Bahae et al [32]. Here the closed(Fig.13 a) and open aperture(Fig.13 b) configurations are discussed connected to the measurable quantities nonlinear absorption (NLA) and nonlinear refraction (NLR) associated with the imaginary and real part of the third order nonlinear susceptibility $\chi(3)$, provides information about the properties of the material. In the Z-scan technique used to characterize the AMPBH, He-Ne laser beam (Gaussian beam) of intensity 5mW (λ = 632.8 nm) was employed as a source, with beam diameter 0.5 mm and a convex lens of focal length

30 mm through which a Gaussian beam was passed. In this procedure, the Z-scan depends in the distortions generated in the spatial and temporal profile of input beam passing through the sample. Total transmitted intensity with respect to the radiations at the sample which is being translated is all due to multi-photon absorption may be limited to two-photon absorption. The variation in far field transmittance beam intensity was measured through the closed aperture using a digital power meter (Field Master GS-coherent). The spatial variation of refractive index caused due to the temperature distribution on surface of the crystal leads to phase distortion in incident beam enables to evaluate the phase-shift ($|\Delta\varphi|$) in transmitted beam by the relation,

$$\Delta T_{P-V} = 0.406(1-S)^{0.25}\left|\Delta\Phi_0\right| \qquad [18]$$

Where (ΔT_{P-V}) denotes variance between peak and valley transmission in closed aperture assessment and S is the linear transmittance aperture and is approximated by,

$$S = 1 - \exp\left(\frac{-2r^2}{\omega_a^2}\right). \qquad [19]$$

r_a is the radius of the aperture and ω_a is the beam radius and spot diameter at the aperture subsequently. The nonlinear refractive index (n_2) can be estimated by using the relation:

$$n_2 = \frac{\Delta\Phi_0}{KI_0L_{eff}} \qquad [20]$$

Here $|\varphi|$ represents on axis phase shift, where I_0 is the on-axis irradiance at focus (Z=0) (I_0, the intensity of the laser beam at focus (Z=0) and L_{eff} is the operative thickness of the sample can be determined by

$$L_{eff} = [1-\exp(-\alpha L)]/\alpha \qquad [21]$$

L denotes the sample length, α represents the linear absorption coefficient, and k represents the wave number ($k = 2\pi/\lambda$).

In open aperture(Fig.13 b), the nonlinear transmission of sample without aperture was tallied. This admits us to resolve the nonlinear absorption coefficient β from open aperture signature,

$$\beta = \frac{2\sqrt{2}\Delta T}{I_0 L_{eff}} \qquad [22]$$

Wherefore $\Delta T=1- T_v$, which that T_v specifies valley transmission value in open aperture determination.This parameter discloses negative value for saturation absorption and positive for two photon absorption and hence has an advantage to be utilized for optical power limiting process and signal processing devices[28,33].

The real and imaginary parts of the third order nonlinear optical susceptibility (χ^3) were established using the formula:

$$\mathrm{Re}\,\chi^{(3)}(esu) = \frac{10^{-4}(\varepsilon_0 C^2 n_o^2 n_2)}{\pi}\left(\frac{cm^2}{W}\right) \qquad [23]$$

$$\mathrm{Im}\,\chi^{(3)}(esu) = \frac{10^{-2}(\varepsilon_0 C^2 n_0 \lambda \beta)}{4\pi^2}\left(\frac{cm^2}{W}\right) \qquad [24]$$

Where, ε_0 is the vacuum permittivity($8.8518 \times 10^{-12}\ Fm^{-1}$) and λ is the wavelength of laser.

The third order nonlinear optical susceptibility (χ^3) of the crystal is figured out from the relation:

$$\left|\chi^{(3)}\right| = \sqrt{(\mathrm{Re}(\chi^{(3)}))^2 + (\mathrm{Im}(\chi^{(3)}))^2} \qquad [25]$$

The third order nonlinear parameters values checked from data's and formulas were tabulated in Table 5 for AMPBH.

In normalized transmittance curvature collected from the closed aperture (Fig.13a) Z scan data, we can able to look that peak is followed by valley suggesting that the sign of refraction nonlinearity is negative i.e., self-defocussing. The self-defocussing effect turns out as a result of alteration in refractive index dependence on temperature and hence this property is enforced in the shielding of optical sensor namely night vision devices where IR night-vision couples with IR illumination having spectral range 700-1000nm [29,22].

The nonlinear absorption coefficient (β) value is $0.0209 \times 10^{-4} cm^2 W^{-1}$ and its positive value stipulates that two photon absorption have occured [28].The nonlinear optical properties of AMPBH make it as a capable possible material in the field of optical limiting application.The ratio of closed to open normal transmittance function is portrayed in the Fig. 13(c) and Fig. 13(d).

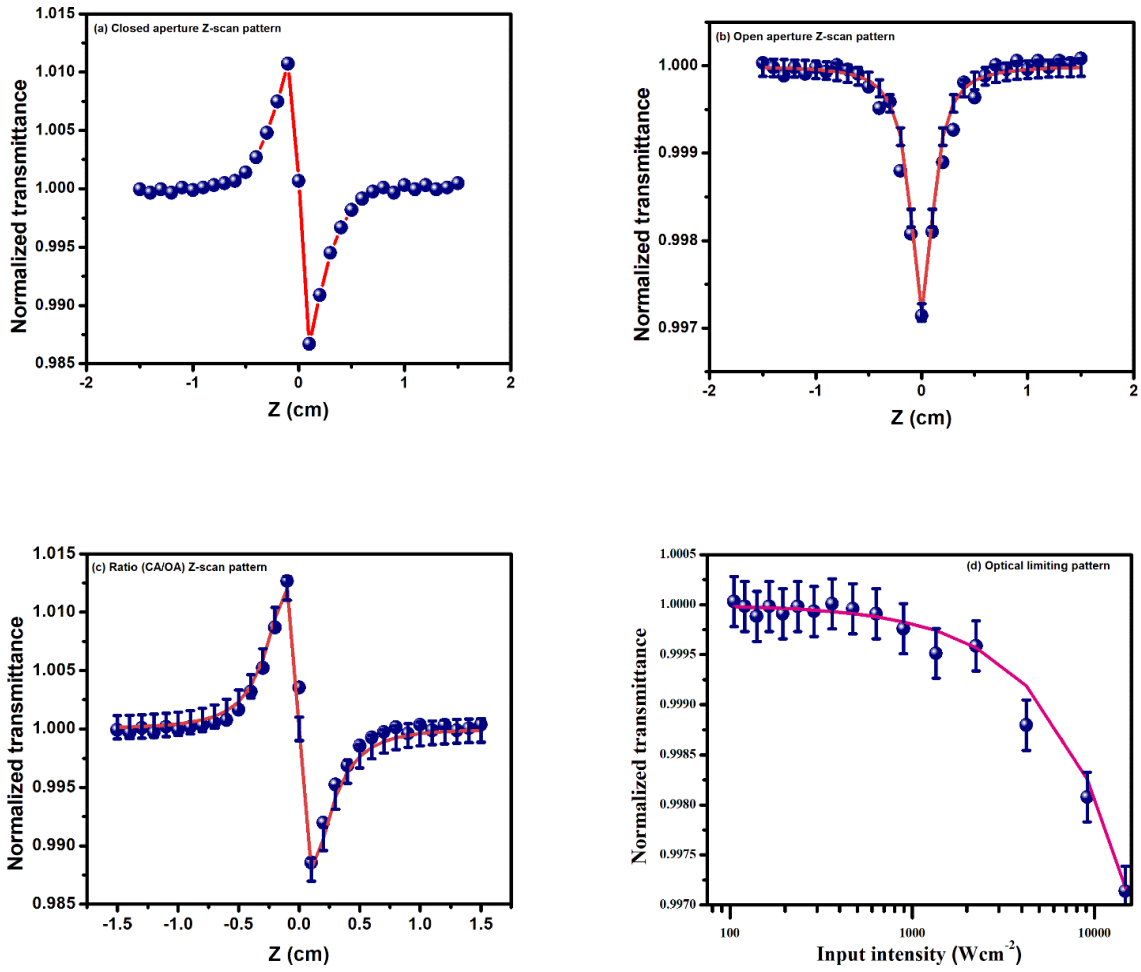

Fig.13. (a,b,c,d) Closed aperture profile , Open aperture profile, Ratio of closed to open z-scan traces , Normalized transmittance versus Input Intensity of AMPBH

Table 5: Obtained nonlinear optical parameters from Z-scan measurements of AMPBH

Third-order nonlinear properties	Measured values
Nonlinear refractive index (n_2)	3.726×10^{-10} cm^2W^{-1}
Nonlinear absorption coefficient (β)	$0.0209 \times 10^{-4} cm^2W^{-1}$
Real susceptibility (χ^3)	1.739×10^{-8} esu
Imaginary susceptibility (χ^3)	4.129×10^{-8} esu
Absolute susceptibility (χ^3)	4.480×10^{-8} esu

4.Conclusion

The alkaline borate symmetric AMPBH crystals were grown and harvested in three weeks by slow evaporation method. The lattice parameters of AMPBH was known from single crystal x-ray diffraction study and found to possess monoclinic system with centrosymmetric space group. FTIR and FT-Raman spectral study established the functional groups comprising the crystal. The evaluated optical parameters from UV-Vis spectral data clearly suggest the alkaline borate material could be utilized in optoelectronics and fabrication of devices. AMPBH is thermally stable up to 125 ˚C which was revealed from TG/DTA analyses. The low dielectric constant and dielectric loss of AMPBH in the high frequency region shows good optical quality. PL spectral profile exhibit sharp green fluorescent peaks at 506 nm, 463 nm and at 384 nm corresponding to green and violet fluorescence spectra. The microhardness Vickers test concludes that the title alkaline borate crystal falls under soft material category. The nonlinear refractive index (n_2), absorption coefficient (β) and third-order nonlinear susceptibility χ^3, (4.480×10^{-8} esu) calculated from Z-scan along with optical and spectral analyses concludes that the alkaline borate crystal AMPBH could serve as an admirable candidate for opto-electronic, photonic and nonlinear optical applications.

Acknowledgement

The scientific support rendered by sophisticated analytical instrument facility (SAIF), IITM Chennai for single crystal XRD and FTIR characterization technique is gratefully acknowledged. Also the authors

thank for the facilities rendered by Department of Physics, St. Joseph College, Trichy for carrying out Microhardness and PL measurement.

References

1. V Siva, SA Bahadur, A Shameem, S Athimoolam, KU Lakshmi, G Vinitha, Synthesis, structural, vibrational, thermal, dielectric and optical properties of third order nonlinear optical single crystal for optical power limiting applications, Journal of Molecular Structure 1191, (2019) 110-117.
2. Y. Zhang, H. Li, B. Xi, Y. Che, J. Zheng, Materials Chemistry and Physics 108, (2008) 192–195,https://doi.org/10.1016/j.matchemphys.2007.09.006.
3. AN Vigneshwaran, P Umarani, C Ramachandra Raja, Studies on nonlinear optical ammonium pentaborate crystals,Journal of Materials Science: Materials in Electronics 28 (15), (2017) 11430-11438.
4. Ömer Şahin, Nasrettin Genli, Mustafa Özdemir. The role of transport processes in crystallization kinetics of ammonium pentaborate. Journal of Crystal Growth, 253 (1-4), (2003) 488-495. https://doi.org/10.1016/S0022-0248(03)01090-X.
5. Fan Zhang, De-Zhongshen, Guang – Qiushen and Xiao – Qing, Crystal structure of cadmium dizinc diborate,CdZn2(BO3)2, Z.Kristallogr.NCS223 (2008) 3-4/DOI10.1524/ncrs.2008.0002.
6. A. Majchrowski, A. Wojciechowski, I.V. Kityk, M. Chrunik, L.R. Jaroszewicz, E. Michalski. Photoinduced nonlinear optical effects in Nd-doped δ-BiB3O6 crystals.Journal of Alloys and Compounds, 610,(2014) 82-85. https://doi.org/10.1016/j.jallcom.2014.04.207.
7. Chen, C.T.; Liu, G.Z. Recent Advances in Nonlinear Optical and Electro-Optical Materials. Annu. Rev.Mater. Sci.16, (1986)203–243.
8. R.Y. Shen, The Principles of Nonlinear Optics, Wiley, New York, 1984.
9. Chen Chuang-tian, W.U. Yi-cheng, L.I. Ru-kang, The relationship between the structural type of anionic group and SHG effect in boron–oxygen compounds, Chin. Phys. Lett. 2 (9) (1985) 389–392.
10. T. Chen, L. Bai, Z.Z. Wang, R.K. Li, Development of new NLO crystals for UV and IR applications J. Cryst. Growth 292, (2006) 169– 178.

11. W.R. Cook, H. Jaffe, The crystallographic, elastic and piezoelectric properties of ammonium pentaborate and potassium pentaborate, Acta Cryst.10, (1957) 705-707.
12. C. Chen, W. Yicheng, L. Rukang, The anionic group theory of the non-linear optical effect and its applications in the development of new high-quality NLO crystals in the borate series, International Reviews in Physical Chemistry,Volume 8, (1989) - Issue 1, 65–9.
13. Zhanggui Hu, Naoki Ushiyama, Yoke Khin Yap, Masashi Yoshimura, Yusuke Mori Takatomo Sasaki, The crystal growth and nonlinear optical properties of K2Al 2B 2O7, Journal of Crystal Growth 237(1) (2002) 654-657.
14. Xiaoyu Dong , Qun Jing, Yunjing Shi, Zhihua Yang, Shilie Pan, Kenneth R Poeppelmeier, Joshua Young, James M Rondinelli, Pb2Ba3(BO3)3Cl: A Material with Large SHG Enhancement Activated by Pb-Chelated BO3 Groups, Journal of the American Chemical Society, 137, (2015) 9417 – 9422.
15. Chunmei Huang, Fangfang Zhang, Bingbing Zhang, Zhihua Yang, Shillie Pan, ”NH4B11O16(OH)2: A New Ammonium Borate with Wavy-Shaped Polycyclic $\infty^2[B_{11}O_{16}(OH_2)]$Layers”,New J of Chemistry, the Royal Society of Chemistry, (2018) Issue 14,DOI:10.1039/x0xx00000x.
16. DA Köse, B Zümreoglu-Karan, T Hökelek, E Sahin, A New Sodium Borate: $Na[B_6O_8(OH)_3]\cdot 6H_2O\cdot H_3BO_3$, Z. Anorg. Allg. Chem., 635, (2009) 563-566.
17. T. Balakrishnan, G.Bhagavannarayana, K.Ramamurthy, Growth,structural , optical, thermal and mechanical properties of ammonium pentaborate crystal, Science Direct,71(2008) 578-583.
18. L.Anandaraj, L.Jothi, Effect of shock waves on enhancing the optical properties of Ammonium Pentaborate Hexahydrate Single crystal Molecular Structure. J.of Mol. Struct. (2021), Doi.org/10.1016/j.molstruc.2021.130068.
19. S. Sudha, M. Peer Mohamed, G.Vinitha, C. Rathika Thaya Kumari, P. Sangeetha,M. Lydia Caroline, ‘Synthesis, growth and third order nonlinear optical studies of a rhombohedral crystal: sodium tetraborate pentahydrate’, Chinese J. Physics, 57,(2019) 211-225.
20. F. Urbach, The Long-Wavelength Edge of Photographic Sensitivity and of the Electronic

Absorption of Solids. Phys.Rev.92 (1953) 1324.

21. M.Nageshwari, C.Rathika Thaya Kumari,S.Sudha, G.Vinitha, M.Lydia Caroline, G.Mathubala, A.Manikandan,'Spectral,dielectric,mechanical and optical chracteristics of LPDMCL single crystal for nonlinear optical applications' Physics B. 582 (2020) 411980.

22. Jonscher A.K., Nature, The 'universal' dielectric response, 267 (1977) 673-679.

23. A.Dilli Rani, C.Rathika Thaya Kumari, M.Nageshwari, P.Sangeetha, G.Vinitha, M.Lydia Caroline, S.Kumaresan, Crystal growth and properties of pure L-alanine and boric acid doped L-alanine nonlinear optical single crystals for frequency conversion,J Mater Sci:Mater Electron, 34 (2023) 280.

24. Sangwal K, On the reverse indentation size effect and microhardness measurement of solids, Materials Chemistry and Physics, 63, (2000) 45-152.

25. Gong, J., Miano, H., Zhao, Z and Guan, Z., , Load-dependence of the measured hardness of Ti(C,N)-based cerments, Material Science Engineering A, 303, (2001) 179-186.

26. Onitsch, E.M., Uber die Mikroharte der Metalle, Mikroscopia, 2, (1947) 131-151.

27. Wooster, W. A., Physical Properties and Atomic Arrangements in Crystals, Reports on Progress in Physics, 16, (1953) 62-82.

28. M Nageshwari, CRT Kumari,P.Sangeetha, G Vinitha, M Lydia Caroline, Third order nonlinear optical, spectral, dielectric, laser damage threshold, and photo luminescence characteristics of an efficacious semiorganic acentric crystal: L-Ornithine monohydrochloride Chinese journal of physics 56 (2),(2018) 502-519.

29. M Nageshwari, P Jayaprakash, CRT Kumari, G Vinitha, M Lydia Caroline,Growth,spectral, linear and nonlinear optical characteristics of an efficient semiorganic acentric crystal: L-valinium L-valine chloridePhysica B: Condensed Matter 511, (2017)1-9.

30. Yuxiang Song, Junpeng Wang, Ling Chen, Ping Yang, Ammonium pentaborate crystals with adjustable and bright phosphorescence and long lifetime, Journal of Luminescence 225 (2020) 117325.

31. C Rathika Thaya Kumari, M Nageshwari, P Jayaprakash, P Sangeetha, S Sudha, M.Lydia Caroline,Investigation on growth, optical, thermal, mechanical, dielectric, LDT studies of sulphanilic

acid monohydrate: A promising third-order nonlinear optical material, Journal of Nonlinear Optical Physics & Materials,26 (2017) 1750020.

[32] M Sheik-Bahae, AA Said, EW Van Stryland, Sheik-Bakhae High-sensitivity, single-beam n2 measurements,Optics letters 14 (17), 955-957.

[33] T.Thilak, M. Basheer Ahamed, G.Vinitha, Third order nonlinear optical properties of potassium dichromate single crystals by Z-scan technique, Optik 124 (2013) 4716–4720.